Bending: from thin interfaces to molecular films in microemulsions

Jean-François Dufrêche, Thomas Zemb

Bending: from thin interfaces to molecular films in microemulsions

J.-F. Dufrêche[a], Th. Zemb[a,*]

[a]*ICSM, University of Montpellier, CEA, CNRS, ENSCM, Marcoule, France*

Abstract

Surfactant film rigidity is a ubiquitous general concept that is quantified in two different units. We show here how to convert the bending rigidity from reduced units of a virtual infinitely thin film (not made of molecules) into the chemical unit ($kJ.mol^{-1}$) of a realistic film of monomolecular thickness. In most cases molecular lengths are not negligible versus curvature radius. Two bending constants for the elasticity of thin-shelled solids can be defined, as introduced by Gauss, whereas only one physical bending constant taking into account that the film cannot be torn has been introduced in the nineties by Hyde and Ninham. The explicit conversion depends on the topology and is different in the quasi-planar approximation, as well as the "direct" o/w or "reverse" w/o case of spherical or cylindrical micelles. We show some examples for classical and nonclassical micelles and microemulsions of different compositions.

Keywords: `elsarticle.cls`, LaTeX, Elsevier, template

2010 MSC: 00-01, 99-00

1. Introduction

Initial understanding of amphiphilic self-assembly started in the seventies with the qualification of the possible formation of curved films made from assembled cones[1]. Entropy was taken only as the mechanism responsible of an

---

*Corresponding author
Email address:* `thomas.zemb@icsm.fr` (Th. Zemb)

effective length of chains averaged over all possible configurations [2]. The fundamental quantity that is used in any model of molecular films has been defined as the packing parameter p. Later, this packing parameter slowly got his index as spontaneous packing parameter p_0, as triggered by molecular shape and intermolecular forces [3]:

$$p_0 = \frac{V_m}{a_0 \langle L \rangle} \tag{1}$$

$\langle L \rangle$ is the average length of the carbon chains. The area per molecule a_0 is the area that minimizes the free energy, *i.e.* the experimentally accessible area in a real sample, but not the area determined in a lattice by crystallography [4]. The volume V_m is safely taken as the molar volume of chains by addition of group contributions [5]. Another method consists in taking the volume of the molecule minus the volume of the head group. The latter is taken by subtraction of partial volumes measured and taking into account the number of physi-sorbed water molecules [6]. This approximation can be applied in all cases except the case of fatty acids and hydroxide-based lipids and surfactants, since partial molar volumes of dissociated H^+ or OH^- may become negative upon dissociation from the head-group[7].

The chain length $\langle L \rangle$ is another expression that hides some uncertainties when it comes to evaluation. In the general literature, the length was taken as the extended chain length. Since the eighties, it was realized that the thermal averaged conformation of chains was important, due to the simple and efficient statistical approach introduced by C. Tanford [8]: whenever an aliphatic chain is considered, the Tanford approximation using for the effective chain 80% of the extended chain length as the effective chain length provides excellent first approximation for size of micelles and microemulsions as observed by scattering. The best predictive general model taking into account entropy of chains is due to Nagarajan [9].

These first attempts towards a predictive theory of phase maps dating from the seventies triggered an immense experimental effort. Using scattering on absolute scale and also extending the scattering angle to high-q region corre-

2

sponding to high resolution resulted in the joint knowledge from experiment of
the absolute values of the area per head-group as well as volume of aggregates
[10]. It was quickly obvious that effective interfacial area per surfactant or lipid
, denoted by σ in experiments and that we will call a in this work was differ-
ent in practice from the spontaneous one a_0 [11]. Hence, an effective packing
parameter can be derived out of SANS/SAXS scattering in any single-phase
micellar or microemulsion:

$$p = \frac{V_m}{a\langle L \rangle} \tag{2}$$

The area a that minimizes the total free energy is the experimentally accessible
area while the spontaneous area a_0 is the area that minimizes the free energy for
one molecule. The shape of the graph linking free energy versus effective area
has been derived for several systems containing amphiphiles [4]. An erroneous
evaluation of p taking the area in the hydrated crystalline form as a value for the
effective or spontaneous area per molecule has been propagated in the literature
and is due to sketches of molecules in a given conformation and without water
bound on head-groups embedded in cylinders and cones.

The distinction between the spontaneous packing parameter p_0 that is a
property of ternary or quaternary systems and the effective packing parameter
p that is a microstructural feature of a given composition is significant. It avoids
confusions due to the use of vague unspecified terms as "packing", "curvature",
or "critical packing parameter". According to Griffin's idea, an emulsifier that is
lipophilic in character is assigned a low Hydrophilic-Lipophilic Balance number
(HLB) and an emulsifier that is hydrophilic in character is assigned a high
HLB number. The mid-point of that scale when used for alkyl ethoxylated
surfactants is ten ($p_0 = 1$). Numerically, initially HLB $= E/5$, where E is
the weight percentage of oxyethylene content. This was extended via a group
contribution to relative water and oil solubility for which the explicit formula
was the algebraic sum of group contributions [12] plus seven. In that scale, at
room temperature, HLB $= 15$ corresponds to a spontaneous packing parameter
of $p_0 = 0.4$ [13].

The reliable group method and scale for HLB (and therefore p_0) was extended [14, 15]. As noticed by Kunieda and Shinoda [16, 17] the w/o or o/w structure was strongly dependent of temperature. Hence the HLB was no more an intrinsic property of a given surfactant and solvent, but a property linked to a special temperature. For nonionic surfactant, the oil solubility quickly decreases with an increase in the number of ethoxy groups of the polar part. It was also noted that the HLB depends linearly on temperature around the Phase Inversion Temperature (PIT) for which HLB is "optimal" (and HLB set to 1 or 10 depending on the authors [14, 15, 16, 17]). The PIT is also known by the name of "balanced temperature" for which $p_0 = 1$. In addition to the size of the polar part, it also depends on the nature of the oil. It was also quantified by the notion of Equivalent Alkane Carbon Number (EACN) that takes into account partial solvent penetration and mixing within the chains of the surfactant. Tables of the effect of solvent penetration are available [18]. Finally, since salinity plays a role in the area per molecule due to the Debye screening of charges in the head-group, the idea of HLB was extended including salt and cosurfactant effects in a so-called Hydrophilic-Lipophilic Difference (HLD) that now depends on the composition and salinity. For a given composition and nature of oil, there is always a temperature for which the Debye screening compensates the headgroup dehydration. In these conditions, HLD = 0, HLB = 7 and $p_0 = 1$. As noticed initially by Kunieda and Shinoda [16], temperature and salinity can compensate. A convenient way to easily distinguish between spontaneous (intrinsic) and effective (sample dependent) packings is to make cuts through phase prisms at constant content of surfactant, by varying the polar volume fraction in the sample [17]. Spontaneous packing parameter p_0 is important in ternary systems, and also valid in binary systems for which it has been initially proposed. The difference between effective and spontaneous parameter HLD [19] has been efficiently extended into the concept of HLD-NAC (Net-Average Curvature) by Acosta *et al.* [20].

The next step towards a predictive description was to assume that the mismatch between effective and spontaneous packing of an incompressible film of

4

molecular thickness that cannot be torn should be approximated by an elastic
free energy that is [21, 22, 23]

$$F_{\mathrm{MFM}} = N \frac{k^\star}{2} (p - p_0)^2 \qquad (3)$$

where N is the number of molecules in the film. We will call this model "Molec-
ular Film Model" (MFM). $k^\star (p - p_0)^2$ is the frustration bending free energy per
molecule. It is expressed in J (per particle), but can be equivalently expressed
in kJ.mol^{-1} by multiplying it by $10^{-3} N_A$ in order to be linked to a chemical
potential term. The same remark can be made for the bending parameter $k^\star$.
Considering the number of particles per unit of surface area $n_s = 1/a$, F_{MFM}
can be expressed as an integral over the surface S:

$$F_{\mathrm{MFM}} = \iint n_s \frac{k^\star}{2} (p - p_0)^2 \, \mathrm{d}S. \qquad (4)$$

This approach allowed the immediate build-up of a molecular theory of curvature
elasticity in surfactant films in a seeding paper that is still in use implicitly or
explicitly in hundreds of papers [24].

The validity of this MFM approach corresponds to the one of the packing
parameter p. The spontaneous geometry of the surfactant molecules is supposed
to be described by this single parameter. Very often, the polar part is more rigid
and much smaller than the carbon chains. Thus, the free energy corresponds
to the reorganization of the chains in the environment. Molecular dynamics
simulations can justify [25] this expression (4). The harmonic approximation is
found to be valid as long as the variation of p are not too important (typically
less than 10-20 %).

Sometimes, when co-surfactants are present, neither the area per molecule
nor the surfactant film thickness are known. In the field of oil recovery mi-
croemulsions are formed with at least three times more molecules of pentanol or
hexanol than the actual surfactants used in the formulation of the microemul-
sions [26, 27, 28]. In these cases, neither the area per molecule nor the surfactant
film thickness is known. Unlocated "neutral bending planes" of an infinitely thin
interface located somewhere in the surfactant monolayer of unknown amount per

5

unit volume of sample and the associated elasticity were defined in $k_\mathrm{B}T$ unit of energy. This proved useful in cases for which entropy as well as enthalpy originating in bending energy could be easily evaluated. Only two phase diagrams could be predicted within this approximation, expressing entropy as well as film bending in reduced units. Also, the predicted scattering peak position is wrong except the degenerate case where oil and water volumes are equal [29]. In these cases where the area per molecule and the surfactant film thickness are not taken into account for the interface description, the MFM is replaced by a Thin Film Model (TFM) for which the interface is only characterized by the radii of curvatures. Mathematically, the TFM has some advantages since it is an expansion valid at low curvature *i.e.* when curvature radii are much larger than the molecular film thickness. This "locally lamellar" case (also called "low curvature"or high internal phase microemulsion (HIPM) or asymmetric sponge) corresponds to the situation where $p - 1 \to 0$. In this case, the expressions introduced by Gauss in differential geometry valid for thin shells and initially developed for describing smectic liquid crystals and stacks of bilayers were extended to slightly bent monolayers by Helfrich [30, 31, 32] in the case of flexible microemulsions [33]. In this case, the free energy is approximated as :

$$F_{\mathrm{TFM}} = \iint \left[\frac{\kappa}{2}(c_1 + c_2 - 2c_0)^2 + \bar{\kappa}c_1 c_2 \right] \mathrm{d}S \qquad (5)$$

where c_1 and c_2 are the local principal curvatures. These Gaussian curvatures are split like in the MFM, in a "spontaneous" and an "effective" value. The mean curvature $\frac{c_1 + c_2}{2}$ is considered and it is very important because it is linked to the preferred number of first neighbours in the film: this number can be more than 6 or less than six, leading to droplet or saddle-splay morphologies [34]. Traditionally, the role of the Gaussian curvature $c_1 c_2$ is neglected: handles and genus of volumes are considered to have negligible impact on free energy. Within this thin film approximation, the two bending constants κ and $\bar{\kappa}$ are energies and can be expressed in $k_\mathrm{B}T$. These two bending constants κ and $\bar{\kappa}$ are not independent from each other, since the condition of untearable film must be met [35]. Mathematical relations become simpler and have been described

6

in detail by Safran [36]. c_0 represents the spontaneous curvature of the film.

Within the MFM, the bending constant $k^\star$ is expressed in units of kJ.mol^{-1} or $k_{\mathrm{B}}T$ per molecule and therefore are additive to chemical potentials. Predictions can be compared explicitly to physical properties related to formulation of micelles and microemulsions. Within the TFM, bending constants κ and $\bar{\kappa}$ are not extensive quantities since they are related to the free energy per unit of surface. These reduced units are also used sometimes in reporting results of MFM experimental studies and mixed up with molecular quantities due to the fact that the order of magnitude is between 3 and 30 $k_{\mathrm{B}}T$ in MFM as well as TFM model context.

The Helfrich expression (5) used in the TFM corresponds to the expansion of the free energy as a function of the local curvatures c_1 and c_2. More precisely, it corresponds to first and second order terms. A constant zeroth order term can be added; it is generally omitted because it can be included in the surface tension. Thus, the expression is valid if the interface is thin, in the sense that the radii of curvatures $1/c_1$ and $1/c_2$ have to be much higher than the molecular scales. Similarly, the spontaneous curvature term $1/c_0$ should also be large in order to apply eq. (5). Nevertheless, this condition is not rigorously necessary. If $1/c_0$ is close to the molecular scale, the Helfrich expression can still be used if c_1 and c_2 are small enough, but c_0 cannot be interpreted in terms of spontaneous curvatures, because if the interface is bent up to this value for c_1 and c_2, higher-order terms become important, and there is no guarantee that the free energy is still minimum for this curvature c_0.

The aim of this review is to define precisely the frustration free energy and express it either within MFM theory or TFM approximation. The conversion of the TFM model characterized by c_0, κ and $\bar{\kappa}$ to the MFM model characterized by p_0 and $k^\star$ depends on the topology. The conversion formulae and the corresponding graphs are given to allow a easy conversion between the two models. Finally, some consequences in understanding literature on water poor w/o aggregates will be given.

2. Theory of frustration energy in reduced and chemical units

The relation between the MFM free energy given by eq. (4) and the TFM free energy given by eq. (5) depends on the considered geometry. Let us calculate these relations for the geometries represented in Figure 1. The location of the interface is represented by a red line. Throughout these theoretical calculations, the curvatures c_1 and c_2 will be counted positive in the direction of the confined phase. Thus in any case, $c_1 > 0$ and $c_2 > 0$, but the sign convention depends on the geometry (positive curvature towards water for inverse micelles and positive curvature towards oil for direct micelles).

Case a) corresponds to a spherical inverse micelle. In that case, $p_0 > 1$. Considering the sign convention of the curvatures, $c_0 > 0$. The aqueous part corresponds to the aqueous phase together with the polar heads. It is embedded in a spherical shell of radius R_1. Beyond R_1 there is the organic (oil) phase. The carbon chain of the amphiphilic molecules at the interface are in a spherical shell between R_1 and $R_2 = R_1 + \delta$. The latter distance $\delta = R_2 - R_1 = \langle L \rangle$ is the average length of the carbon chains. The relation between the two free energies (4) and (5) is obtained by identifying the expression around the equilibrium state (for which F_{TFM} and F_{MFM} are minimum) when R_1 varies. For the spherical inverse micelle represented in Fig. 1 a), the TFM free energy (5) reads

$$F_{\text{TFM}}^a = 8\pi\kappa(1 - c_0 R_1)^2 + 4\pi\bar{\kappa}. \tag{6}$$

The MFM free energy (4) is

$$F_{\text{MFM}}^a = \frac{4\pi R_1^2 n_s k^\star}{2}\left(1 + \frac{\delta}{R_1} + \frac{\delta^2}{3R_1^2} - p_0\right)^2. \tag{7}$$

Both formula (6) and(7) yield a minimum as functions of R_1. The values of R_1 for which the free energies are minimum follow respectively $c_0 R_1 = 1$ for (6) and $p_0 = 1 + \frac{\delta}{R_1} + \frac{\delta^2}{3R_1^2}$ for (7). Therefore the relation between the spontaneous curvature c_0 of the TFM and the spontaneous packing parameter p_0 of the MFM reads:

$$p_0 = 1 + c_0\delta + \frac{1}{3}c_0^2\delta^2. \tag{8}$$

8

In the same way the identification of the second derivatives $\frac{\mathrm{d}^2 F^a}{\mathrm{d}R_1^2}$ around this minimum yields the relation between the bending parameters:

$$k^\star = \frac{4\kappa}{n_s \delta^2} \frac{1}{(1 + \frac{2}{3}\delta c_0)^2}. \tag{9}$$

These relations between (c_0,κ) and $(p_0,k^\star)$ are given in Table 1 together with the inverse formula. The Gaussian bending parameter $\bar{\kappa}$ cannot be obtained in that case because it only corresponds to a constant term in the free energy (6). Indeed, the Gauss-Bonnet theorem allows the direct calculation of the Gaussian curvature term in eq. (5) for a compact surface:

$$\iint \bar{\kappa} c_1 c_2 \, \mathrm{d}S = 2\pi \bar{\kappa} \chi \tag{10}$$

where χ is the Euler characteristic of the surface ($\chi = 2$ for a sphere). The role of $\bar{\kappa}$ consists in adding a term which only depends on the topology of the surface. Thus it cannot be obtained from a procedure for which the latter is constant.

It should be emphasized that the equivalence between the two formula (4) and (5) obtained here is calculated for a given number of particles per unit of surface area n_s and a given chain length δ. Indeed the two parameters are assumed to be constant when the shape of the surface is modified. The exact values of n_s and δ depend on further terms in the free energy. As a matter of fact, the minimization which defines the equivalece of the two models is not a global physical minimization of the free energy. Surfactant molecules are added or removed when the radius change and they are taken from a state where they have their spontaneous shape for which the free energy is assumed to be zero. This reference state is valid for the comparison of the two formula (4) and (5) because it is the same, but in a real system it does not exist: the surfactants have to be taken from another state so that the global free energy minimum may correspond to another geometry. A similar remark can be made for the amount of the aqueous phase incorporated in the polar core which depends on the radius R_1.

For a system for which the spontaneous curvature is zero ($c_0 = 0 \iff p_0 =$

9

1), the TFM yields a somewhat paradoxical result. Indeed, the free energy (6) becomes $F^a_{\text{TFM}} = 4\pi(2\kappa + \bar{\kappa})$ so that the frustration is mathematically independent on the radius! Bigger spheres have more surfaces and therefore more surfactants but they are less curved so the two effects compensate each other exactly. On the other hand, in the frame of the MFM, the corresponding free energy (7) reads $F^a_{\text{MFM}} = 2\pi n_s k^\star \delta^2 \left(1 + \frac{\delta}{3R_1}\right)^2$. The frustration increases with the curvature. Correspondingly small reverse micelles are difficult to obtain due to their large cost in kJ.mol^{-1}.

A similar calculation can be done for a cylindrical inverse micelle represented in Fig. 1 b). In that case the two free energies (per unit of length) are

$$f^b_{\text{TFM}} = \frac{\pi\kappa}{R_1}(1 - 2c_0 R_1)^2 \tag{11}$$

and

$$f^b_{\text{MFM}} = \frac{2\pi R_1 n_s k^\star}{2}\left(1 + \frac{\delta}{2R_1} - p_0\right)^2. \tag{12}$$

The identification of the radius R_1 for which the free energies are minimum and the identification of the second derivatives yields:

$$p_0 = 1 + c_0\delta \tag{13}$$

and

$$k^\star = \frac{4\kappa}{n_s\delta^2}. \tag{14}$$

These relations between (c_0,κ) and $(p_0,k^\star)$ for a cylindrical inverse micelle are given in Table 1 together with the inverse formula.

The calculation in the case of the same geometries, spherical and cylindrical, can also be done for direct micelles represented in Fig. 1 c) and d). In that case, $p_0 < 1$ (but we still have $c_0 > 0$ because of the sign convention for the curvatures). The identification of the two free energies thus gives in the same way the link between the parameters of the two models. The results are also presented in Table 1 for both directions of conversion. Again, as the surface topology is not changed in the minimization procedure, it is not possible to obtain an expression for $\bar{\kappa}$.

10

The situation is different if we consider a general surface characterized by the mean and the Gaussian curvature $H = \frac{1}{2}(c_1 + c_2)$ and $K = c_1 c_2$. The situation is represented in Fig. 1 e). The local packing parameter p of the interface molecules is related to the volume confined at a distance δ from the interface. Following Gauss theorem, a small surface S at the interface, when translated perpendicularly at a distance x from the interface in the direction of oil is modified and becomes:

$$S' = S(1 + 2Hx + Kx^2) \tag{15}$$

By integration between $x = 0$ for which the surface is S to $x = \delta$ for which the surface is $S' = S(1 + 2H\delta + K\delta^2)$ we get the estimated molecular volume of the chains:

$$V_m = \int_0^\delta S(x)\,\mathrm{d}x = S\left(\delta + H\delta^2 + K\frac{\delta^3}{3}\right). \tag{16}$$

Hence

$$p = \frac{V_m}{S\delta} = 1 + H\delta + K\frac{\delta^2}{3}. \tag{17}$$

The resulting MFM free energy (4) per unit of surface is

$$f_{\mathrm{MFM}}^e = \frac{n_s k^\star}{2}\left(1 + H\delta + K\frac{\delta^2}{3} - p_0\right)^2. \tag{18}$$

The corresponding TFM free energy (5) per unit of surface reads

$$f_{\mathrm{TFM}}^e = 2\kappa(H - c_0)^2 + \bar{\kappa}K = 2\kappa H^2 + 2\kappa c_0^2 - 4\kappa c_0 H + \bar{\kappa}K. \tag{19}$$

where the curvature sign convention is the one of inverse micelles (positive curvature toward water). The two equations (18) and (19) are not exactly equivalent. The constant terms correspond to surface tension so that they do not give information for the curvature effects but there are further differences. Following the original derivation by Helfrich, the equation (19) can be understood as an expansion of the free energy as a function of the curvatures for which only the linear and quadratic terms in H, H^2 and K are considered. Such terms are also present in (18) together with higher order terms proportional to K^2 or HK. These terms are beyond the TFM. By identification of the terms proportional

11

to H, H^2 and K in (18) and (19) we obtain the following general expression linking the coefficients of the two models:

$$p_0 = 1 + c_0 \delta \quad \text{and} \quad k^\star = \frac{4\kappa}{n_s \delta^2} = -\frac{3\bar{\kappa}}{n_s c_0 \delta^3} \tag{20}$$

In the opposite sign convention for the curvature (positive curvature toward oil), we have

$$p_0 = 1 - c_0 \delta \quad \text{and} \quad k^\star = \frac{4\kappa}{n_s \delta^2} = \frac{3\bar{\kappa}}{n_s c_0 \delta^3} \tag{21}$$

These relations between $(c_0, \kappa, \bar{\kappa})$ and $(p_0, k^\star)$ for a general surface (in the limit of low curvature which is the one of Helfrich free energy (5)) are given in Table 1 together with the inverse formula. In any case, a relation between the mean bending rigidity and the Gaussian bending rigidity is obtained:

$$4(p_0 - 1)\kappa + 3\bar{\kappa} = 0 \tag{22}$$

κ and $\bar{\kappa}$ have opposite signs for inverse micelles $p_0 > 1$. In that case, $\bar{\kappa} < 0$. The Gauss-Bonnet theorem implies that separated small micelles are preferred. On the other hand, for direct micelles, $p_0 < 1$, $\bar{\kappa} > 0$ and bicontinuous microemulsions are preferred. For a flat interface, as indicated in Table 1, the Gaussian bending rigidity is zero: $\bar{\kappa} = 0$.

The MFM predicts a relation between the two bending constants κ and $\bar{\kappa}$ of the Helfrich Hamiltonian used in the TFM. If the MFM is valid, only two physical quantities are enough to characterize bending of interfaces. Therefore, a relation exists between the three quantities that define the Helfrich free energy. It should be noted that this relation (22) does not belong to the Helfrich description. A molecular parameter is necessary to link κ and $\bar{\kappa}$ (it can either be p_0 or δ). This prediction of the MFM can hardly be tested because of the difficulty to measure $\bar{\kappa}$, though. In the most precise determination of bending constants available up to now in the literature, light scattering, neutron scattering as well as surface tension were used jointly in a known phase diagram and for a known specific area of water/oil contact area per unit volume of same: even in this case [37], only the experimental value of $2\kappa + \bar{\kappa}$ could be measured.

12

The relations between the parameters of the TFM model $(c_0, \kappa, \bar{\kappa})$ and the one of the MFM $(p_0, k^\star)$ are represented in Fig. 2. Globally the cylindrical geometry coincides with the case of general surfaces. The bending energies $k^\star$ and κ are in that case directly proportional. They are equal if the area per molecule $a_0 = 1/n_s$ is $\delta^2/4$. The spherical case magnifies the dependence in $c_0\delta$. The spontaneous curvature c_0 is typically in the order of $1/\delta$. When $\delta \to 0$, the molecular film is thin, and the spontaneous curvature can be very large.

As long as $c_0\delta$ is not negligible, the link between the two models depends on the geometry. Spheres are not equivalent to cylinders. The difference comes from the fact that when $1/c_0 \approx \delta$ the Helfrich Hamiltonian used in the TFM in not valid when the curvature is around c_0 because the curvature radii are not bigger than the molecular length δ. There is a possibility of inconsistency when the same Helfrich parameters are used for all the geometries. The MFM is free of this problem.

3. Current state of knowledge

The theoretical section described the link between the infinitely thin film model TFM and the more realistic molecular film model MFM. The generality of a model can be evaluated via the predictive power on all distinct observables that can be experimentally determined [11]. In the case of microemulsions, these are mainly:

- the phase diagrams of phase prisms versus several projections. Triangular phase cuts at constant temperature or surfactant to co-surfactant ratio that are supposed to be made for constant spontaneous packing, "fish-cut" , "chi-cuts" , "Lund cuts" or formulator's cut have been established, sometimes in great details by identifying tie-lines. Three dimensional representations with regions with two and three phases are very difficult to draw since tie lines and triangles coexist. Initiated by Shinoda[17] in the seventies, three different "cuts" of the phase prism became common practice: a triangle for constant spontaneous packing determination, the "fish

13

Inverse Microemulsions: Curvature toward Water $\quad p_0 > 1$		
Sphere	$p_0 = 1 + c_0\delta + \frac{1}{3}c_0^2\delta^2 \quad \Longleftrightarrow \quad c_0 = \frac{1}{2\delta}\left(\sqrt{12p_0 - 3} - 3\right)$ $k^\star = \frac{4\kappa}{n_s\delta^2}\frac{1}{(1+\frac{2}{3}\delta c_0)^2} \quad \Longleftrightarrow \quad \kappa = \frac{n_s\delta^2 k^\star}{3}\left(p_0 - \frac{1}{4}\right)$		
Cylinder	$p_0 = 1 + c_0\delta \quad\quad\quad\quad\quad \Longleftrightarrow \quad c_0 = \frac{p_0 - 1}{\delta}$ $k^\star = \frac{4\kappa}{n_s\delta^2} \quad\quad\quad\quad\quad\quad \Longleftrightarrow \quad \kappa = \frac{n_s\delta^2 k^\star}{4}$		
General	$p_0 = 1 + c_0\delta \quad\quad\quad\quad\quad \Longleftrightarrow \quad c_0 = \frac{p_0 - 1}{\delta}$ $k^\star = \frac{4\kappa}{n_s\delta^2} = -\frac{3\bar\kappa}{n_s c_0\delta^3} \quad \Longleftrightarrow \quad \kappa = \frac{n_s\delta^2 k^\star}{4} \text{ and } \bar\kappa = \frac{n_s\delta^2(1-p0)k^\star}{3}$ $4c_0\delta\kappa + 3\bar\kappa = 0 \iff 4(p_0 - 1)\kappa + 3\bar\kappa = 0$		
Direct Microemulsions: Curvature toward Oil $\quad p_0 < 1$		
Sphere	$p_0 = 1 - c_0\delta + \frac{1}{3}c_0^2\delta^2 \quad \Longleftrightarrow \quad c_0 = \frac{1}{2\delta}\left(3 - \sqrt{12p_0 - 3}\right)$ $k^\star = \frac{4\kappa}{n_s\delta^2}\frac{1}{(1-\frac{2}{3}\delta c_0)^2} \quad \Longleftrightarrow \quad \kappa = \frac{n_s\delta^2 k^\star}{3}\left(p_0 - \frac{1}{4}\right)$		
Cylinder	$p_0 = 1 - c_0\delta \quad\quad\quad\quad\quad \Longleftrightarrow \quad c_0 = \frac{1 - p_0}{\delta}$ $k^\star = \frac{4\kappa}{n_s\delta^2} \quad\quad\quad\quad\quad\quad \Longleftrightarrow \quad \kappa = \frac{n_s\delta^2 k^\star}{4}$		
General	$p_0 = 1 - c_0\delta \quad\quad\quad\quad\quad \Longleftrightarrow \quad c_0 = \frac{1 - p_0}{\delta}$ $k^\star = \frac{4\kappa}{n_s\delta^2} = \frac{3\bar\kappa}{n_s c_0\delta^3} \quad \Longleftrightarrow \quad \kappa = \frac{n_s\delta^2 k^\star}{4} \text{ and } \bar\kappa = \frac{n_s\delta^2(1-p0)k^\star}{3}$ $-4c_0\delta\kappa + 3\bar\kappa = 0 \iff 4(p_0 - 1)\kappa + 3\bar\kappa = 0$		
Flat interface: $\quad p_0 = 1$		
In all Cases	$p_0 = 1 \quad\quad\quad\quad\quad\quad\quad \Longleftrightarrow \quad c_0 = 0$ $k^\star = \frac{4\kappa}{n_s\delta^2} \quad\quad\quad\quad\quad\quad \Longleftrightarrow \quad \kappa = \frac{n_s\delta^2 k^\star}{4} \text{ and } \bar\kappa = 0$		

Table 1: Link between the parameters c_0, κ, and $\bar\kappa$ of Thin Film Model (TFM; based on the Helfrich Hamiltonian and on the concept of curvature) and the parameters p_0 and $k^\star$ of the Molecular Film Model (MFM; based on the concept of packing parameter p). By convention, the spontaneous curvature c_0 is counted positively towards water in the case of direct systems and towards oil in the case of reverse systems. Thus we always have $c_0 > 0$.

cut" when determination of phase inversion temperature and efficiency is searched for, and the chi-cut which enhances the differences between effective and spontaneous packing.

- the neutron (SANS) or X-ray scattering patterns [38]

- the electrical conductivity , as well as molecular diffusion coefficients de-

14

termined by NMR [39]

Other quantities, such as viscosity, turbidity, ultra-sound absorption, osmometry, surface tensions [40] are less frequently reported in a systematic way, but still relevant to test models.

A useful classification of the different classes of ternary solutions containing at least one surface active component is the distinction between rigid ($k^\star >$ 10 kJ.mol^{-1}) , flexible ($k^\star = 1 - 10$ kJ.mol^{-1}), ultra-flexible (UFME) and "poorly structured microemulsions". In the two latter, the bending of the surfactant film does not play a detectable role. In the first one, temperature effects are not dominant and therefore film bending does not play a role. The TFM as well as the MFM are useful only to the class of flexible microemulsions.

Using ternary phase diagrams combined to scattering (peak position, power-laws at extrema as well as absolute cross-sections) is the most stringent test for the validity of the prediction of a model. Moreover, most experimental tests have been made in the degenerated case of 50% water and 50% oil where most derivatives cancel.

The most popular experimental system is the one of hydrocarbon polyethoxy-lates CiEj linear surfactants. The most studied case is when "j " is approximately half of "i". This ensures that $c_0.\delta \approx 0$, as is HLD. The temperature is a convenient way to vary spontaneous curvature, as in the fish-cut established by Strey and co-workers [41], or in triangular cuts at constant temperature introduced in the seventies by Per Ekwall and co-workers [42], or in the Lund-cut [43]. The fish cut keeps water and oil volumes equal while the Lund-cut is plotted versus active materials, $i.e$ versus solvent plus solute. The Phase inversion Temperature (PIT) with minimal amount of surfactant and equal amount of water is easy to determine. At this point, the spontaneous packing parameter as well as the effective packing parameter are both close to one. Near this balanced PIT point, the TFM expansion is approximately valid, provided that the curvature radius of the interface is large versus the interfacial thickness that can therefore be determined.

15

When curvature frustration and entropy of the film are the two only mechanisms competing, and in the absence of any other source of chemical potential, the Helfrich approximation of the TFM, originally devoted to bilayers can be used as a fair approximation. To our best knowledge, the ternary phase diagram resembles qualitatively to the one predicted by the MFM model for the "universal" case of the special surfactant C10E4 picked out at 44.6 °C ±1 °C and with octane as the oil [44]. Only in this case, the only phase competing with the microemulsions is an oil-swollen lamellar phase. Close the PIT temperature and with nearly equal amounts of water and oil, the position of scattering peak is predicted by Milner and co-workers [45], but it fails by 20% for other water/oil ratio. Another reason for failure of prediction of the TFM is the usage of Helfrich approximation when curvature radii are only two to three times larger than film thickness (*i.e.* surfactant length). The expansion in curvature is only valid in practice when the concentration of surfactant is at most a few g.L^{-1} : to our best knowledge, this situation where Helfrich approximation is valid has been obtained experimentally only once in the thousands of papers describing microemulsions, using the ultra-long non-ionic surfactant C16E6 [46].

In all other cases, some other chemical or long range enthalpic or entropic mechanism come into play, and the TFM fails. The MFM model associated to a quadratic form of the free energy of bending is the only one who can be compared to experimental results. As a first general success of the MFM model, local microstructures such as connected cylinders or locally lamellar microstructures [47, 48] that are predicted by the MFM model (but not by the TFM model) have been clearly identified in the ternary phase diagram [49]. This extraordinary success has helped to popularize cuts in phase prism, and the distinction between spontaneous and effective packing in the formulation of microemulsions. The formulation rules were found to formulate microemulsions using lipids associated to co-surfactants for pharmacy [50], as well as formulation in cosmetics and home-care including only components allowed and still incorporating large amounts of fragrances in microemulsions [51].

All these progresses were based on determination of the stiffness of the inter-

face, and hence the resilience of the formulation versus added solutes. Added solutes can modify the volume fraction as well as the area per surfactant molecule, and hence the spontaneous packing: this has been demonstrated by Pileni and co-workers [52].

The table 2 below lists the available values for all the bending constant established in the literature up to now. They are given in kJ.mol^{-1}. The experimental method of investigation used is also indicated in the Table. Contrary to the available determinations of the monolayer bending rigidity, there are only very few experimental evaluations of spontaneous packing: only the points for which $p_0 = 1$, (or HLD= 0 in chemical engineering literature) are known. So a general test of TFM is not yet possible in the current state of knowledge. This is in our opinion, a domain that will expand quickly , due to its industrial importance.

Surfactant	$a_0 = 1/n_s$ nm^2	κ $k_B T$	$\delta = V_c/a_0$ nm	$k^\star$ $k_B T$ and kJ.mol^{-1}	$c_0\delta$	Source
C6E2 in n-octane	0.42	0.44 persistence length	0.48	3.2 8.0 kJ.mol^{-1}	≈ 0	[53]
C8E3 in n-octane	0.48	0.57 persistence length	0.53	3.9 9.7 kJ.mol^{-1}	≈ 0	[53]
C10E4 in n-octane	**0.54**	**0.73** persistence length	**0.56**	**5.0** **12.5 kJ.mol^{-1}**	≈ 0	[54] [53]
C12E5 in n-octane	0.60	0.92 persistence length	0.59	6.3 15.6 kJ.mol^{-1}	≈ 0	[53]
C12 generic	0.40	2 molecular modelling	1.8	1.0 2.4 kJ.mol^{-1}	?	[24]
W/O microemulsion AOT/water/isooctane	*0.58*	*0.5 - 5* *inconsistent with* *phase diagram*	*1*	*0.78 - 7.8* *1.9 - 19 kJ.mol^{-1}*	*0.33*	[55] [56]
DMPC monolayer (29C)	0.7	0.56 $\pm$0.06 hexagonal swelling	1.53	0.67 1.7 kJ.mol^{-1}	≈ 0	[57]
SDS monolayer O/W	*0.7* *co-surfactant* *quantity unknown*	1.22 cubic swelling	*2*	*0.96* *2.4 kJ.mol^{-1}*	0.5	[58]
TDMAO/octanol/decane d$_{22}$/D$_2$O generic	0.5	2.5 droplet polydispersity	1.24	16 40 kJ.mol^{-1}	0.83	[37]
+pentanol (unknown mole ratio)	0.7	1 droplet polydispersity	1.22	3.8 9.5 kJ.mol^{-1}	0.2	
Water/DDAB/cyclohexane in diluted regime W/O spheres	0.7	0.5 droplet polydispersity	*1.1*	*0.65* *1.6 kJ.mol^{-1}*	*0.5*	[59]
Water/DDAB/dodecane W/O cylinders	0.7	> 3.3 phase boundary	1.8	> 2.9 7.1 kJ.mol^{-1}	0.2	[60]
Water/DDAB/tetradecane quasi planar	0.7	> 3.3 phase boundary	1.8	> 2.9 7.1 kJ.mol^{-1}	0.1	[61]

Table 2: Summary of published values for bending constants determined within the infinitely film model (TFM) and the molecular film model (MFM). Conversion of κ in reduced units related to bending of a virtual bent surface located at an unknown position of the neutral plane to chemical quantities $k^\star$ which can be used to calculate macroscopic quantities such as the phase diagrams (kJ.mol^{-1}). This conversion requires the knowledge of the molecular volume, the area per molecule a_0, the molecular film thickness δ, as well as the dimensionless product $c_0.\delta$ that is assumed to be vanishing within the Helfrich approximation of the TFM. Values given in the Table are shown in bold for the reference (most studied) case and in italic when not derived directly within the reference, but deduced from general knowledge.

4. Application to water poor systems

Water-poor solutions of surfactants in non-polar solvents have been considered since a long -time under the name of reverse or inverse micelles [62]. When no water molecules are present, the binary solution should be considered as "reverse" micelles if the solution is shown as being more structured than a regular solution. The existence of "true" reverse micelles has been questioned, since the presence of one or more water molecules per w/o micelle is needed to observe detectable scattering coming from 4-6 molecules in the most known case (Dioctyl sodium sulfosuccinate, AOT). In common laboratory experiments, these "reverse micelle" are present as an extremely hygroscopic ternary solution that even desiccates saturated calcium chloride: the equilibrium relative humidity is so low that obtaining water-free solutions of AOT requires a glove box and highly controlled dry atmosphere [62]. When water is present, the governing quantity is the water/surfactant mole ratio [56].

In all cases described with the two most popular examples Na-AOT or sodium di(2-ethylhexyl) phosphate (Na-DEHP), when $w \leqslant 3$ water molecules per surfactant, the most accurate designation would be swollen reverse micelles. Since water molecules are bound as a first hydration layer of the surfactant head-groups, they do not move faster than the whole aggregate, no "internal fluid" is detected [6]. The true microemulsion regime (*i.e.* an internal fluid separated from the apolar solvent by an interfacial film) only start with $w > 3$ water molecules per surfactant. The easy access to purified AOT and H-DEHP induces an enormous literature (more than 1500 papers since the initial ones [63] by K Shinoda and H.F. Eicke). What is so special about AOT is that the spontaneous curvature concept must be taken with care [64]. The chains are branched, meaning a large entropic contribution to frustration and the area per head-group varies by more than 25% if the head-group is uncharged or the counter-ion dissociated. As a result, large domains of water-conducting lamellar phases coexist not only with sponge phases, but also with closed w/o "droplet-like" more or less coalesced dispersions at the same temperature. In reduced

19

units, the bending constant is of the order of $k_{\mathrm{B}}T$, making AOT a perfect example of a flexible microemulsion, but with a spontaneous curvature not controlled by temperature, but by the dissociation of the sulfo-succinate head-group, *i.e.* by the presence of added salts [65]. As a result of the knowledge of bending energy in the presence of electrolytes as expressed in the MFM context, AOT is the first system for which solubilization of electrolytes, such as amino-acids has been measured [66, 67] and quantitatively understood [68, 69]. Water-poor reverse aggregates of oil-soluble surfactants made of 4 to 20 molecules or even bicontinuous connected cylinder structures are at the core of the vast majority of liquid-liquid extraction as well as phase-transfer catalytic processes [70].

These water-poor aggregates do not correspond to true microemulsions, however the interfacial film is bent and we are frequently in the case where $c_0.\delta > 1$: the TFM approximation do not hold and the MFM concept of frustration of a thick and bent monolayer has to be considered. Using the MFM, the first maps of probability of occurrence of aggregates containing N extractant molecules and H water molecules in the core of each aggregate could be deduced from the free energy dependence of the composition, using the harmonic expression of the frustration energy versus packing as a scalar. The valley of stability expressed by the weak w/o aggregation free energy in (N,H) coordinates for the popular diamide extractant is shown in figure 3a. Figure 3b shows the resulting distribution map. These distribution maps predict the "polydispersity" that is linked to strong dampening in small-angle X-ray scattering (SAXS) and in small angle neutron scattering (SANS) at high q, as well as the persistent differences in aggregation numbers when measured by osmometry or scattering in absolute scale [71, 72].

The weak w/o aggregates made of less than ten molecules are not easy to characterise by SANS or SAXS, since the size of an aggregate is not clearly different from the size of a molecule: the procedure of removing an arbitrary "solvent" containing only monomers used in scattering evaluation is no more precise. The main strategy is the comparison of scattering as predicted by Molecular dynamics to the scattering observed experimentally [73].

20

Duvail and co-workers have shown that within the MFM model, the wetting by the solvent has to be considered explicitly in order to obtain harmonic expression of free energy versus packing [25]. In the case of diamides containing lanthanides, a value for $k^\star$ within the MFM of 40 kJ.mol^{-1} with a spontaneous packing of $p_0 = 4.0$ is obtained. Such a high-value of p_0 explains that large hydrated ions are less extracted than small dehydrated ions [74]. Three hydrocarbon chains or less cannot determine any "internal" volume. The case of six chains in an aggregate made by three associated diamides has been considered [75], comparing short and long alkanes: "penetrating" or wetting solvents induce an increase of the spontaneous packing parameter as well as a slight increase in the bending constant. Figure 4 shows as an example, a trimer with nine hydrocarbon chains wet by three different solvents. In the representation showing carbons at their location versus center of gravity as black dots; the stronger wetting of low mass alkanes of the chains that is visible in the figure is also responsible of the stronger resilience versus third phase formation in real processes that require process intensification [76].

The studies described up to now aggregates made by one kind of extractant. It is well known in practice that using two extractants at an optimal mole ratio allows extraction to be magnified by a factor 10 to 30 in efficiency as well as selectivity. Solvent penetration in the highly curved surfactant film has been shown to be part of the effect [77]. A general theory linking the observed maximum of extraction to to the maximum of mixing free energy close to equimolarity has been published very recently [78]. However, the enthalpic part that can be evaluated from MD or even semi-analytically within the droplet model should be investigated more. Figure 5 illustrates how the presence of trivalent cations in the core of a reverse aggregate can change the microstructure from globular reverse micelles to elongated structures that eventually connect and induce strong changes in electrical conductivity of extractant solutions [79]. Even in the case of multivalent cations, specific effects beyond electrostatics are of the same order of magnitude as surfactant-film frustration of bending and cannot be ignored to understand liquid-liquid extraction[80].

21

5. Conclusion and outlook

Stiff and ultra-flexible microemulsions do not depend on a delicate balance between enthalpy and entropy, since they are dominated by solvation terms and steric hindrance. The most common ones in industrial application are the flexible ones, when $\kappa^\star$ is between 2 and 20 kJ.mol^{-1}. They are also the most described ones in academic work.

We stress here that the condition that $c_0\delta \approx 0$ in order to be able to use the Helfrich expansion is indeed very demanding. If one considers that the assumption is valid if $c_0\delta < 0.1$, in one dimension, this means that the radius of "internal" fluid nanodroplets is ten times larger than the surfactant length. In three dimension, it means that the volume of the droplet must be less than 0.1%: so the surfactant content is less than 0.1%. If the expansion of $c_0.\delta$ is accepted when it is less than 0.3, then the surfactant content should be less than 3%: these conditions have hardly ever been achieved. The single example [46] for which the specific area is also known has been given by Ishikawa et al. in 2016. In this case, the harmonic expression for packing is consistent with the scattering observed for flexible microemulsions, but not for ultra-flexible and stiff microemulsions [38].

The scattering peak position is only predicted close to 50 % volume fraction of water, where most models converge to the same value. Observations about surfactants with complex flexible head-groups can only be explained with two bending constants. Predictive modelling able to also predict scattering, phase sequence and boundaries along dilution lines is still in its infancy. Why?

The first reason is that the spontaneous packing is taken as a scalar, independent of ionic strength, counter-ion release and adsorption of co-surfactant. Huge variations of $k^\star$ and p_0 versus surface charge have been predicted twenty years ago, but not yet verified experimentally [81]. As a consequence, no phase prism have yet been superposed to free energy maps. The initial propositions of perturbing ions by Leontidis [82] and antagonistic salts by Onuki [83] had recently found a clear experimental verification [84]. Another reason is that most

22

academic studies have been focused on a few molecular structures ($C_jE_{i/2}$, SDS + co-surfactant, DDAX, AOT...). When the headgroups are large as in the case of alkylglucosides, the model with a single bending constant is not valid and compatible with the non-spherical character of the diluted micelles [85]. A extended MFM treatment dealing with two bending constants is mandatory.

Ubiquitous microemulsions heavily used in pharmacy, cosmetics, food industry and cleaning industry are more mysterious than stars. Adding in the same unit (kJ.mol^{-1}), solvation, mixing entropy within given topological constraints may however produce soon the first predicted phase prism cut that resembles to an experimentally determined one. In any case this would require calculation of bending free energy in kJ.mol^{-1} as a function of a few measurable quantities.

6. Acknowledgements

Recommended reading

• of special interest

•• of outstanding interest

[21] • This paper explains how a harmonic expression for bending frustration energy has to take into account that molecular length cannot be neglected versus curvature radii. Moreover, the fact that amphiphilic films cannot be torn is

[560] required to explain sequences of phases as well as morphologies observed semi-quantitively for the first time.

[22] • Similarly to ref. [21] , but focused on microemulsions with molecular size taken into account.

[23] • Prediction of morphology for stiff and flexible microemulsions in asymmetric volume fraction.

[24] •• Seeding paper showing that molecular sizes, applied to the hydrocarbon thickness only, show the way to the derivation of free energy related to bending, including entropy. This work addresses lots of questions still open as today, even if more than hundred studies were based on the premises shown here.

[29] • First experimental confirmation that prediction of peak position based on Helfrich expansion at $c_0 \delta$ of the order of 1 and at knowwn persistence length fail in predicting the observed scattering spectra far from 50% volume partition.

[46] •• The first experimental example of a degenerated case close to 50% water-oil volume with small spontaneous curvature larger than film thickness. In that case, the Helfrich expansion and equation of state are used to derive a phase diagram and scattering properties that resemble closely to the experimental ones.

[48] • The position of the scattering peak of a microemulsion, as well as the effect of local bending constraint of instability experimentally observed are theoretically predicted for the first time using Gaussian Random Waves.

[56] •• The first complete quantitative evaluation of free energy for a ternary microemulsion, making a complete theory starting form initial questioning forty years ago, by H.F. Eicke [62] and M. Borkovec [55].

[37] • Experimental proof of the effect on bending energy controlled by addition of co-surfactant at a given mole fraction. This effect is now at the basis of a vast number of practical formulations.

[71] • The explicit derivation of a free energy valley of stability of water-poor reverse micelles, explaining the long known discrepancy between osmotic and scattering measures of average mass.

24

References

[1] J. N. Israelachvili, D. J. Mitchell, B. W. Ninham, Theory of Self-Assembly of Hydrocarbon Amphiphiles Into Micelles and Bilayers, Journal of the Chemical Society, Faraday Transactions 2 72 (1976) 1525–1568.

[2] C. Tanford, The Hydrophobic Effect: Formation of Micelles and Biological Membranes 2d Ed, John Wiley & Sons, 1980.

[3] K. A. Dill, S. Bromberg, Molecular Driving Forces, Garland Science, 2010.

[4] P. Bauduin, T. Zemb, Perpendicular and lateral equations of state in layered systems of amphiphiles, Current Opinion in Colloid & Interface Science 19 (1) (2014) 9–16.

[5] A. Immirzi, B. Perini, Prediction of density in organic crystals, Acta Crystallographica Section A: Crystal Physics, Diffraction, Theoretical and General Crystallography 33 (1) (1977) 216–218.

[6] M. Freda, G. Onori, A. Paciaroni, A. Santucci, Hydration and dynamics of aerosol OT reverse micelles, Journal of molecular liquids 101 (1-3) (2002) 55–68.

[7] O. Regev, C. Kang, A. Khan, Cryo-TEM and NMR Studies of Solution Microstructures of Double-Tailed Surfactant Systems: Didodecyldimethylammonium Hydroxide, Acetate, and Sulfate, The Journal of Physical Chemistry 98 (26) (1994) 6619–6625.

[8] C. Tanford, Y. Nozaki, M. F. Rohde, Size and shape of globular micelles formed in aqueous solution by n-alkyl polyoxyethylene ethers, The Journal of Physical Chemistry 81 (1977) 1555–1560.

[9] R. Nagarajan, Molecular Packing Parameter and Surfactant Self-Assembly: The Neglected Role of the Surfactant Tail, Langmuir 18 (2001) 31–38.

25

[10] S. H. Chen, Interactions and phase transitions in micellar and microemulsion systems studied by small angle neutron scattering, Physica B+C 137 (1-3) (1986) 183–193.

[11] Y. Chevalier, T. Zemb, The structure of micelles and microemulsions, Reports on Progress in Physics 53 (3) (1999) 279–371.

[12] Attwood D and Florence A, Surfactant Systems: Their Chemistry, Pharmacy and Biology, Chapman and Hall, 1983.

[13] B. W. Berger, R. Y. García, A. M. Lenhoff, E. W. Kaler, C. R. Robinson, Relating surfactant properties to activity and solubilization of the human adenosine a3 receptor, Biophysical Journal 89 (1) (2005) 452 – 464.

[14] I. J. Lin, L. Marszall, Partition coefficient, HLB and effective chain length of surface-active agents, in: Emulsions, Steinkopff, Heidelberg, Heidelberg, 1978, pp. 99–104.

[15] I. J. Lin, L. Marszall, Cmc, HLB, and Effective Chain-Length of Surface-Active Anionic and Cationic Substances Containing Oxyethylene Groups, Journal of colloid and interface science 57 (1) (1976) 85–93.

[16] H. Kunieda, K. Shinoda, Phase-Behavior in Systems of Non-Ionic Surfactant - Water Oil Around the Hydrophile-Lipophile-Balance-Temperature (Hlb-Temperature), Journal of Dispersion Science and Technology 3 (3) (1982) 233–244.

[17] K. Shinoda, Solution Behavior of Surfactants - the Importance of Surfactant Phase and the Continuous Change in Hlb of Surfactant, Progress in Colloid and Polymer Science 68 (1983) 1–7.

[18] S. Queste, J. Salager, R. Strey, J.-M. Aubry, The EACN scale for oil classification revisited thanks to fish diagrams, Journal of colloid and interface science 312 (1) (2007) 98–107.

[19] J. F. Ontiveros, C. Pierlot, M. Catté, V. Molinier, J.-L. Salager, J.-M. Aubry, A simple method to assess the hydrophilic lipophilic balance of food and cosmetic surfactants using the phase inversion temperature of c10e4/n-octane/water emulsions, Colloids and Surfaces A: Physicochemical and Engineering Aspects 458 (2014) 32 – 39.

[20] E. J. Acosta, The HLD-NAC equation of state for microemulsions formulated with nonionic alcohol ethoxylate and alkylphenol ethoxylate surfactants, Colloids and Surfaces A: Physicochemical and Engineering Aspects 320 (1-3) (2008) 193–204.

[21] S. T. Hyde, Curvature and the Global Structure of Interfaces in Surfactant-Water Systems, Journal De Physique 51 (23) (1990) C7209–C7228.

[22] S. T. Hyde, I. S. Barnes, B. W. Ninham, Curvature Energy of Surfactant Interfaces Confined to the Plaquettes of a Cubic Lattice, Langmuir 6 (6) (1990) 1055–1062.

[23] S. T. Hyde, B. W. Ninham, T. Zemb, Phase Boundaries for Ternary Microemulsions - Predictions of a Geometric Model, Journal of Physical Chemistry 93 (4) (1989) 1464–1471.

[24] I. Szleifer, D. Kramer, A. Ben-Shaul, W. M. Gelbart, S. A. Safran, Molecular theory of curvature elasticity in surfactant films, Journal of Chemical Physics 92 (11) (1990) 6800–6817.

[25] M. Duvail, S. van Damme, P. Guilbaud, Y. Chen, T. Zemb, J.-F. Dufrêche, The role of curvature effects in liquid-liquid extraction: assessing organic phase mesoscopic properties from MD simulations, Soft Matter 13 (33) (2017) 5518–5526.

[26] A. M. Bellocq, D. Roux, A Global Description of Phase Equilibria in the Quaternary Microemulsion System: Water-Dodecane-Pentanol-Sodium Dodecylsulfate, in: Progress in Microemulsions, Springer, Boston, MA, Boston, MA, 1989, pp. 159–184.

27

[27] S. E. Friberg, G. Rong, A Nonaqueous Microemulsion System - Formamide, Sodium Dodecyl-Sulfate, Hexanol, and Toluene, Langmuir 4 (4) (1988) 796–801.

[28] N. Nakamura, T. Tagawa, K. Kihara, I. Tobita, H. Kunieda, Phase transition between microemulsion and lamellar liquid crystal, Langmuir 13 (7) (1997) 2001–2006.

[29] O. Abillon, L. T. Lee, D. Langevin, K. Wong, Microemulsions: structures, surfactant layer properties and wetting transitions, Physica A 172 (1991) 209–218.

[30] W. Helfrich, Effect of thermal undulations on the rigidity of fluid membranes and interfaces, Journal De Physique 46 (7) (1985) 1263–1268.

[31] G. Beblik, R. M. Servuss, W. Helfrich, Bilayer Bending Rigidity of Some Synthetic Lecithins, Journal De Physique 46 (10) (1985) 1773–1778.

[32] L. T. Lee, D. Langevin, K. Wong, Microemulsions: experimental aspects, Journal of Physics: Cond. Matt. 2S (1990) SA333–SA338.

[33] D. Andelman, M. E. Cates, D. Roux, S. A. Safran, Structure and phase equilibria of microemulsions, The Journal of chemical physics 87 (12) (1987) 7229.

[34] S. H. Hyde, A. S, K. Larsson, Z. Blum, T. Landh, L. Sven, B. W. Ninham, The Language of Shape , The Role of Curvature in Condensed Matter: Physics, Chemistry and Biology, Elsevier, 1996.

[35] A. Fogden, S. T. Hyde, G. Lundberg, Bending Energy of Surfactant Films, Journal of the Chemical Society, Faraday Transactions 87 (7) (1991) 949–955.

[36] S. A. Safran, Statistical Thermodynamics of Surfaces, Interfaces and Membranes, Addison-Wesley, 1994.

28

[37] M. Gradzielski, Effect of the Cosurfactant Structure on the Bending Elasticity in Nonionic Oil-in-Water Microemulsions, Langmuir 14 (21) (1998) 6037–6044.

[38] S. Prevost, M. Gradzielski, T. Zemb, Self-assembly, phase behaviour and structural behaviour as observed by scattering for classical and non-classical microemulsions, Advances in Colloid and Interface Science 247 (2017) 374–396.

[39] J. Sjoblom, R. Lindberg, S. E. Friberg, Microemulsions - Phase equilibria characterization, structures, applications and chemical reactions, Advances in Colloid and Interface Science 65 (1996) 125–287.

[40] D. Langevin, Micelles and microemulsions, Annual Review of Physical Chemistry 43 (1992) 341–369.

[41] R. Strey, Phase behavior and interfacial curvature in water-oil-surfactant systems, Advances in Colloid and Interface Science 1 (1996) 402–410.

[42] P. Ekwall, L. Mandell, K. Fontell, Solubilization in Micelles and Mesophases and the Transition from Normal to Reversed Structures, Molecular Crystals 8 (1) (2007) 157–213.

[43] M. S. Leaver, U. Olsson, H. Wennerström, R. Strey, U. Wurz, Phase-Behavior and Structure in a Nonionic Surfactant-Oil-Water Mixture, Journal of the Chemical Society, Faraday Transactions 91 (23) (1995) 4269–4274.

[44] R. Strey, On the Stability Range of Microemulsions: From the Tricritical Point to the Lamellar Phase in Water/Formamide-Octane-CiEj Systems, Berichte Der Bunsen-Gesellschaft-Physical Chemistry Chemical Physics 97 (5) (1993) 742–750.

[45] S. T. Milner, S. A. Safran, D. Andelman, M. E. Cates, D. Roux, Correlations and structure factor of bicontinuous microemulsions, Journal De Physique 49 (6) (1988) 1065–1075.

29

[46] K. Ishikawa, M. Behrens, S. Eriksson, D. Topgaard, U. Olsson, H. Wennerström, Microemulsions of Record Low Amphiphile Concentrations Are Affected by the Ambient Gravitational Field, J. Phys. Chem. B 120 (26) (2016) 6074–6079.

[47] M. Duvail, J.-F. Dufrêche, L. Arleth, T. Zemb, Mesoscopic modelling of frustration in microemulsions., Physical chemistry chemical physics 15 (19) (2013) 7133–7141.

[48] M. Duvail, L. Arleth, T. Zemb, J.-F. Dufrêche, Predicting for thermodynamic instabilities in water/oil/surfactant microemulsions: A mesoscopic modelling approach, The Journal of chemical physics 140 (16) (2014) 164711.

[49] U. Olsson, U. Wurz, R. Strey, Cylinders and Bilayers in a Ternary Nonionic Surfactant System, Journal of Physical Chemistry 97 (17) (1993) 4535–4539.

[50] M. J. Lawrence, G. D. Rees, Microemulsion-based media as novel drug delivery systems, Advanced Drug Delivery Reviews 64 (2012) 175–193.

[51] V. Tchakalova, F. Testard, K. Wong, A. Parker, D. Benczédi, T. Zemb, Solubilization and interfacial curvature in microemulsions, Colloids and Surfaces A: Physicochemical and Engineering Aspects 331 (1-2) (2008) 31–39.

[52] M.-P. Pileni, T. Zemb, C. Petit, Solubilization by reverse micelles: Solute localization and structure perturbation, Chemical physics letters 118 (4) (1985) 414–420.

[53] T. Sottmann, R. Strey, S. Chen, A Small-Angle Neutron-Scattering Study of Nonionic Surfactant Molecules at the Water-Oil Interface - Area per Molecule, Microemulsion Domain Size, and Rigidity, The Journal of chemical physics 106 (15) (1997) 6483–6491.

[54] R. Strey, Microemulsion Microstructure and Interfacial Curvature, Colloid & Polymer Science 272 (8) (1994) 1005–1019.

[55] M. Borkovec, Phenomenological theories of globular microemulsions, Advances in Colloid and Interface Science 37 (3-4) (1992) 195–217.

[56] V. F. Razumov, S. A. Tovstun, Statistical Thermodynamics of Water-in-Oil Microemulsions Stabilized with an Ionic Surfactant, Colloid Journal 81 (4) (2019) 337–365.

[57] D. Marsh, Elastic curvature constants of lipid monolayers and bilayers, Chemistry and Physics of Lipids 144 (2) (2006) 146–159.

[58] J. M. Seddon, R. H. Templer, Cubic Phases of Self-Assembled Amphiphilic Aggregates, Philosophical Transactions of the Royal Society of London Series a-Mathematical Physical and Engineering Sciences 344 (1672) (1993) 377–401.

[59] J. E. and, D. Sharpe, R. K. Heenan, S. Egelhaaf, Rigidities of Cationic Surfactant Films in Microemulsions, Journal of Physical Chemistry B 101 (6) (1997) 944–948.

[60] T. N. Zemb, The DOC model of microemulsions: microstructure, scattering, conductivity and phase limits imposed by sterical constraints, Colloids and Surfaces A 129-130 (1997) 435–454.

[61] I. S. Barnes, P.-J. Derian, S. T. Hyde, B. W. Ninham, T. N. Zemb, A disordered lamellar structure in the isotropic phase of a ternary double-chain surfactant system, Journal De Physique 51 (22) (1990) 2605–2628.

[62] H.-F. Eicke H. Christen, Is water critical to the formation of micelles in apolar media?, Helvetica Chimica Acta 61 (1978) 2258.

[63] H. F. Eicke, Surfactants in nonpolar solvents, in: Micelles, Springer-Verlag, Berlin/Heidelberg, 1980, pp. 85–145.

[64] S. Nave, J. Eastoe, J. Penfold, What is so special about aerosol-OT? 1. Aqueous systems, Langmuir 16 (23) (2000) 8733–8740.

[65] J. Meunier, L. T. Lee, Bending elasticity measurements of a surfactant monolayer by ellipsometry and x-ray reflectivity, Langmuir 7 (9) (1991) 1855–1860.

[66] E. B. Leodidis, T. A. Hatton, Amino acids in AOT reversed micelles. 1. Determination of interfacial partition coefficients using the phase-transfer method -, Journal of Physical Chemistry 94 (1990) 6400–6411.

[67] E. B. Leodidis, T. A. Hatton, Amino acids in AOT reversed micelles. 2. The hydrophobic effect and hydrogen bonding as driving forces for interfacial solubilization, The Journal of Physical Chemistry 94 (16) (1990) 6411–6420.

[68] E. B. Leodidis, A. S. Bommarius, T. A. Hatton, Amino acids in reversed micelles. 3. Dependence of the interfacial partition coefficient on excess phase salinity and interfacial curvature, The Journal of Physical Chemistry 95 (15) (1991) 5943–5956.

[69] E. B. Leodidis, T. A. Hatton, Amino acids in reversed micelles. 4. Amino acids as cosurfactants, The Journal of Physical Chemistry 95 (1991) 5957–5965.

[70] T. Zemb, C. Bauer, P. Bauduin, L. Belloni, C. Déjugnat, O. Diat, V. Dubois, J.-F. Dufrêche, S. Dourdain, M. Duvail, C. Larpent, F. Testard, S. Pellet-Rostaing, Recycling metals by controlled transfer of ionic species between complex fluids: en route to "ienaics", Colloid & Polymer Science 293 (1) (2015) 1–22.

[71] M. Bley, B. Siboulet, A. Karmakar, T. Zemb, J.-F. Dufrêche, A predictive model of reverse micelles solubilizing water for solvent extraction, Journal of colloid and interface science 479 (2016) 106–114.

[72] A. Karmakar, M. Duvail, M. Bley, T. Zemb, J.-F. Dufrêche, Combined supramolecular and mesoscale modelling of liquid–liquid extraction of rare

32

805   earth salts, Colloids and Surfaces A: Physicochemical and Engineering Aspects 555 (2018) 713–727.

[73] Ph. Guilbaud Th. Zemb, Solute-induced microstructural transition from weak aggregates towards a curved film of surface-active extractants, ChemPhysChem 13 (2012) 687.

810   [74] S. Gourdin, J.-F. Dufrêche, M. Duvail, T. Zemb, Microemulsion as model to predict free energy of transfer of electrolyte in solvent extraction, submitted.

[75] S. Stemplinger, M. Duvail, J.-F. Dufrêche, The influence of the diluent in liquid-liquid extraction: investigation of eu3+ extraction with dmdohema in n-alkanes microemulsion as model to predict free energy of transfer of electrolyte in solvent extraction, submitted.

[76] L. Berthon, L. Martinet, F. Testard, C. Madic, T. Zemb, Solvent Penetration and Sterical Stabilization of Reverse Aggregates based on the DIAMEX Process Extracting Molecules: Consequences for the Third Phase Formation, Solvent Extraction and Ion Exchange 25 (5) (2007) 545–576.

[77] J. Rey, S. Dourdain, J. F. Dufreche, L. Berthon, J. M. Muller, S. Pellet-Rostaing, T. Zemb, Thermodynamic Description of Synergy in Solvent Extraction: I. Enthalpy of Mixing at the Origin of Synergistic Aggregation, Langmuir 32 (49) (2016) 13095–13105.

825   [78] M. Špadina, K. Bohinc, T. Zemb, J.-F. Dufrêche, Synergistic solvent extraction is driven by entropy, ACS Nano 13 (12) (2019) 13745–13758.

[79] P. Guilbaud, T. Zemb, Depletion of water-in-oil aggregates from poor solvents: Transition from weak aggregates towards reverse micelles, Current Opinion in Colloid & Interface Science 20 (1) (2015) 71–77.

830   [80] V. Mazzini, V. S. J. Craig, Specific-ion effects in non-aqueous systems, Current Opinion in Colloid & Interface Science 23 (2016) 82–93.

33

[81] A. Fogden, B. W. Ninham, Electrostatics of curved fluid membranes: The interplay of direct interactions and fluctuations in charged lamellar phases, Advances in Colloid and Interface Science 83 (1-3) (1999) 85–110.

[82] E. Leontidis, Chaotropic salts interacting with soft matter: Beyond the lyotropic series, Current Opinion in Colloid & Interface Science 23 (2016) 100–109.

[83] A. Onuki, S. Yabunaka, T. Araki, R. Okamoto, Structure formation due to antagonistic salts, Current Opinion in Colloid & Interface Science 22 (2016) 59–64.

[84] M. Hohenschutz, I. Grillo, O. Diat, P. Bauduin, How nano-ions act like ionic surfactants, Angewandte Chemie International edition 59 (2020) 1–6.

[85] C. Cecutti, B. Focher, B. Perly, T. Zemb, Glycolipid self-assembly: micellar structure, Langmuir 7 (1991) 2580–2585.

Figure list
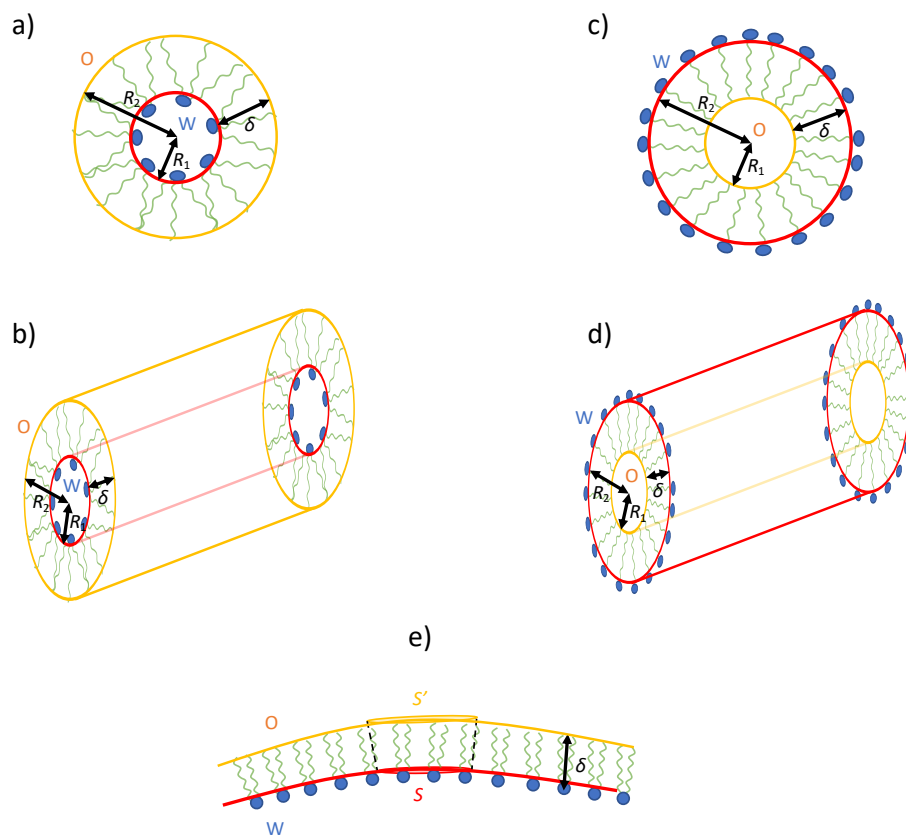
Figure 1: Geometry of the calculated structures. a): spherical inverse micelle, b): cylindrical inverse micelle, c) spherical direct micelle, d) cylindrical direct micelle, e) more general case where any curved interface is considered.
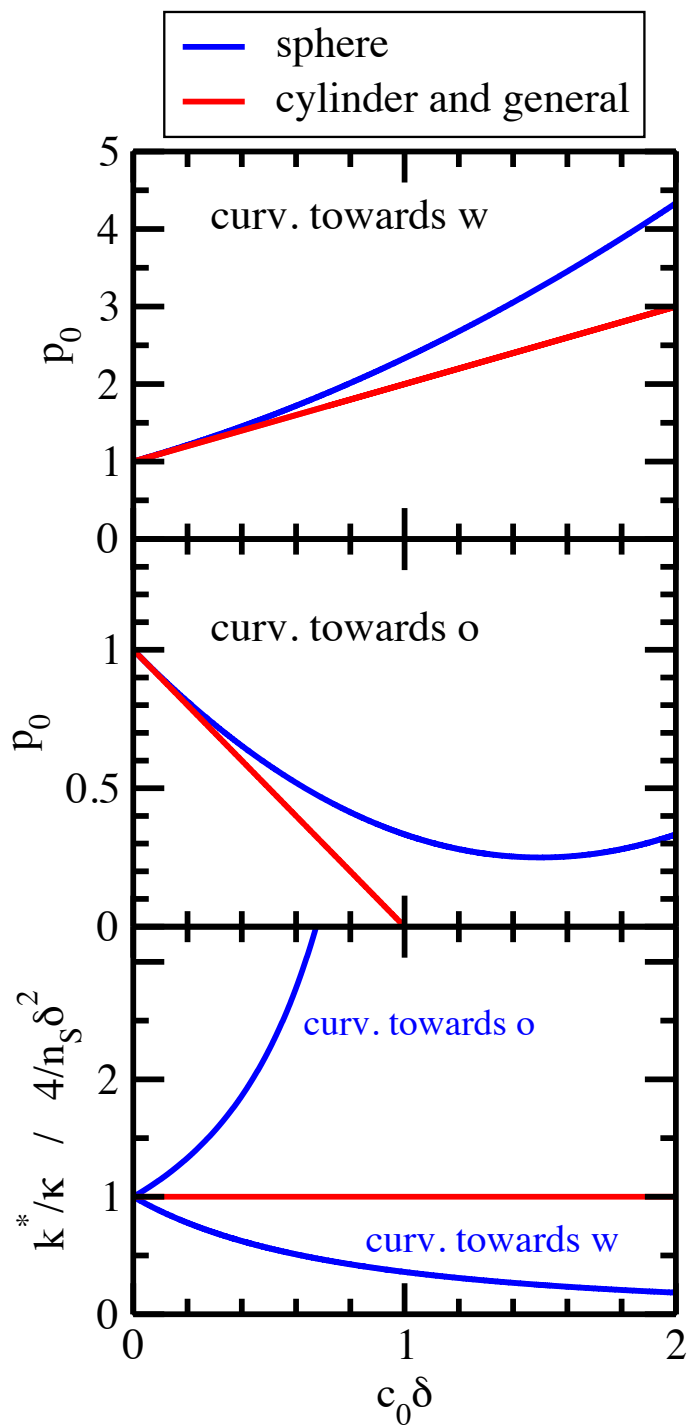
Figure 2: Spontaneous packing parameter p_0 and ratio $k^\star/\kappa$ of the bending energy ($4/n_s\delta^2$ unit) as functions of $c_0\delta$. Inverse microemulsions (curvature towards water) and direct microemulsions (curvature towards oil) cases are represented.
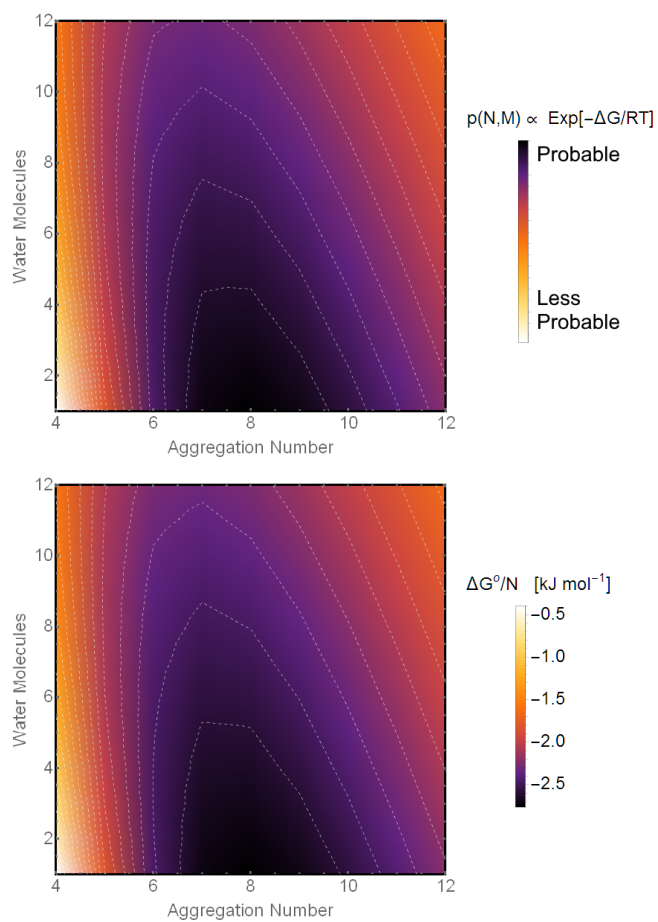
Figure 3: Potential surface of probability distribution (up) and standard Gibbs energy (down) of water/extractant aggregates in oil as functions of the number of water molecules and the number of extractant molecules (aggregation number) in the aggregate [71]. The dashed lines indicate the shape of the valley of stability. Courtesy of M. Bley.
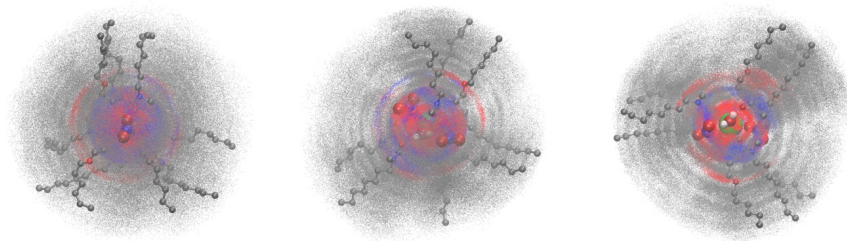
Figure 4: "Cloud" representation of a micelle consisting of Eu^{3+} (green), three nitrates, water and three DMDOHEMA extractant molecules in (left) n-heptane, (middle) n-nonane and (right) n-dodecane. Courtesy of S. Stemplinger and M Duvail.
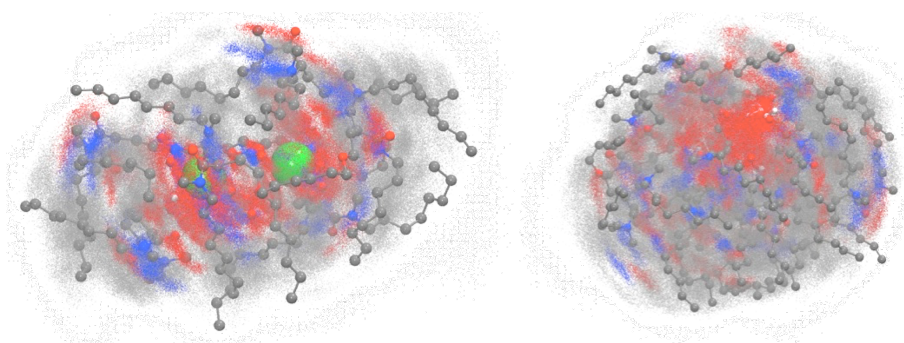

Figure 5: "Cloud" representation of a water poor w/o aggregate in presence (right= $2Eu^{3+}$ + $6 NO_3^-$ + 6 DMDOHEMA + 4 H_2O) or in absence (right=10 DMDOHEMA + 10 H_2O) of an ionic salt. Same color code as in Fig. 4. The polar and non-polar cores are represented through atomic cloud densities, that is, superposition of carbon (light grey), oxygen and nitrogen (dark grey) atoms trajectories obtained by molecular dynamics simulations [73]. Courtesy of Ph. Guilbaud.

Graphical TOC